Inorganic Chemistry

Article

pubs.acs.org/IC

# Hydrothermal Synthesis and Comparative Coordination Chemistry of New Rare-Earth $V^{4+}$ Compounds

Martin M. Kimani, Colin D. McMillen, and Joseph W. Kolis*

Department of Chemistry and Center for Optical Materials Science and Engineering Technologies (COMSET), Clemson University, Clemson, South Carolina 29634-0973, United States

Supporting Information

**ABSTRACT:** Several new hydrated rare earth vanadates and rare earth oxy-vanadates have been synthesized using hydrothermal techniques and characterized using single crystal and powder X-ray diffraction and infrared and UV−vis absorption spectroscopies. The hydrated rare earth vanadates adopt the space group $P2_1/m$ with general formula $A_3VO_5(OH)_3$ (A = Y (**1**), Dy (**2**), or La (**3**)) and contain anionic distorted square pyramidal $[VO_5]^{-6}$ units and $AO_7$ and $AO_8$ polyhedra. The oxy-vanadates with the general formula $A_2O(VO_4)$ (A = Y (**4**), Dy (**5**; **6**), or Yb (**7**)) form two polymorphs in either $P2_1/c$ or $C2/c$ space groups and contain anionic tetrahedral $[VO_4]^{-4}$ units and nonvanadium bonded $O^{2-}$ anions in distorted $[OA_4]$ tetrahedra. In all cases, the vanadium ion is in the tetravalent oxidation state, and its original source was the trace $V^{4+}$ impurities in $YVO_4$. The observed vanadyl and equatorial vanadium−oxygen bond lengths about the square pyramid in compounds **1**−**3** and the tetrahedral vanadium coordination found in compounds **4**−**7** are unusual for $V^{4+}$. The electronic and vibrational spectra are also reported and correlated with the appropriate coordination environment.

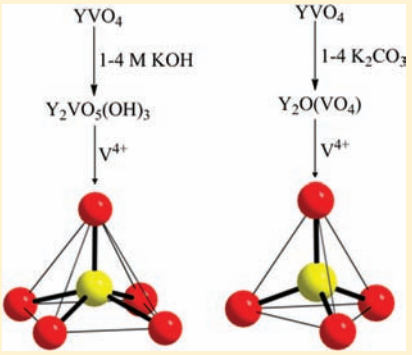


## INTRODUCTION

Yttrium orthovanadate ($YVO_4$) and its derivatives are useful optical materials for solid-state laser applications. Single crystals of lanthanide doped $YVO_4$ (particularly Nd:$YVO_4$) have superior lasing efficiency over materials like Nd:YAG due to an enhanced stimulated emission cross-section and a broader absorption manifold near 808 nm.[1,2] This large stimulated emission cross-section leads to good lasing, and the broad absorption peak enables efficient diode pumping.[3] These factors combine to provide excellent microlaser characteristics as well.[4] Also, the structure of the $YVO_4$ crystal is uniaxial with a significant birefringence, so that all emitted light is polarized, allowing for more efficient Q switching.[5] An excellent summary of the qualities of $YVO_4$ as a laser host was recently provided by Kalisky.[6] Other combinations of dopants (Yb, Er Tm, Ho) and related hosts (i.e $GdVO_4$, $LuVO_4$) are also being explored for specialized lasing applications.[7,8]

In other optical applications of vanadate crystals, $Eu^{3+}$-doped $YVO_4$ has been used as a red phosphor in color televisions and cathode ray tubes, and other different colors such as blue and reddish-orange phosphors can be obtained by doping $YVO_4$ with $Tm^{3+}$ and $Sm^{3+}$, respectively.[9,10] Recent studies have shown potential application of lanthanide-doped $YVO_4$ thin films as luminescent materials in plasma display panels. All of these properties make it important to understand thoroughly the crystal growth and physical properties of the material.

Rare earth vanadate crystals are grown using several methods such as flux,[11] laser heated pedestal growth, top seeded solution growth,[12] floating zone,[13] Czochralski growth,[14] and hydrothermal techniques.[15] However there are a number of problems related to the growth of high optical quality single crystals of $YVO_4$ and its relatives. Foremost is the fact that the material does not strictly melt congruently, so any technique relying on melting $YVO_4$ has challenges in providing high quality crystals. One major issue with high temperature melt growth is the tendency of the $V^{5+}$ ions to become reduced to lower valent $V^{3+}$ and $V^{4+}$ oxidation states at higher temperatures. This creates oxygen defects and absorption bands in the crystal due to the lower valent vanadium ions. This problem can be suppressed by the addition of oxygen to the growth atmosphere, but this leads to oxidation of the crucible and incorporation of metal oxide contaminants in the crystal. The trace amount of lower oxidation state vanadium ions in reduced oxidation states in commercial $YVO_4$ is responsible for the characteristic pale greenish-brown color of the bulk material.

Partly to address these issues of undesirable reduced vanadium oxidation states in the bulk $YVO_4$ crystals, we investigated a hydrothermal route to bulk single crystals of $YVO_4$ and its congeners for commercial optical applications.[15] Whittingham et al. previously reviewed the use of mild hydrothermal methods in the synthesis of a number of vanadium oxides containing organic species or metal cations such as the alkali metals, alkaline earths, zinc, and copper.[16] In addition, Byrappa and Yoshimura previously reported a hydrothermal route to small crystalline $YVO_4$.[17] We were able to develop a route to versatile large single crystals of the lanthanide vanadates, and because of the relatively low growth

Received: November 9, 2011
Published: March 1, 2012

   dx.doi.org/10.1021/ic2024132 | Inorg. Chem. 2012, 51, 3588−3596

Table 1. Crystallographic Data for Compounds 1, 4−7

| | 1 | 4 | 5 | 6 | 7 |
|---|---|---|---|---|---|
| chemical formula | $Y_3VO_5(OH)_3$ | $Y_2VO_5$ | $Dy_2VO_5$ | $Dy_2VO_5$ | $Yb_2VO_5$ |
| fw (g/mol) | 448.69 | 308.76 | 455.94 | 455.94 | 477.02 |
| space group | $P2_1/m$ | $C2/c$ | $P2_1/c$ | $C2/c$ | $C2/c$ |
| temp./K | 293 | 293 | 293 | 293 | 293 |
| cryst syst | monoclinic | monoclinic | monoclinic | monoclinic | monoclinic |
| $a$, Å | 5.5382(11) | 14.435(5) | 9.0699(18) | 14.470(3) | 14.265(3) |
| $b$, Å | 10.301(2) | 6.7344(13) | 6.9545(14) | 6.7521(14) | 6.6826(13) |
| $c$, Å | 5.9197(12) | 10.430(2) | 6.6987(13) | 10.467(2) | 10.274(2) |
| $\alpha$, deg | 90 | 90 | 90 | 90 | 90 |
| $\beta$, deg | 105.30(3) | 122.21(2) | 106.79(3) | 122.14(3) | 121.99 |
| $\gamma$, deg | 90 | 90 | 90 | 90 | 90 |
| $V$, Å$^3$ | 325.73(11) | 857.9(4) | 404.53(14) | 865.9(3) | 830.7(3) |
| $Z$ | 2 | 8 | 4 | 8 | 8 |
| $D_{cal}$, Mg/m$^3$ | 4.575 | 4.781 | 7.486 | 3.497 | 3.814 |
| indices (min) | [−7, −14, −7] | [−17, −8, −12] | [−12, −9, −8] | [−17, −8, −13] | [−17, −8, −12] |
| (max) | [7, 14, 8] | [15, 8, 12] | [12, 8, 8] | [17, 8, 12] | [17, 8, 12] |
| params | 64 | 73 | 74 | 74 | 74 |
| F(000) | 414 | 1128 | 780 | 780 | 812 |
| $\mu$, mm$^{-1}$ | 27.852 | 28.874 | 38.724 | 18.091 | 23.384 |
| $2\theta$ range, deg | 3.57−29.95 | 3.34−25.24 | 2.35−29.59 | 3.33−27.79 | 3.48−26.40 |
| collected reflns | 3368 | 3585 | 3722 | 3571 | 3262 |
| unique reflns | 844 | 774 | 940 | 886 | 824 |
| final $R$ (obs. data),[a] $R_1$ | 0.0395 | 0.0864 | 0.0577 | 0.0413 | 0.0607 |
| $wR_2$ | 0.0930 | 0.2425 | 0.1606 | 0.1293 | 0.1731 |
| final $R$ (all data), $R_1$ | 0.0433 | 0.0980 | 0.0591 | 0.0513 | 0.0686 |
| $wR_2$ | 0.0971 | 0.2602 | 0.1623 | 0.1575 | 0.1973 |
| goodness of fit (S) | 1.081 | 1.145 | 1.106 | 1.204 | 1.199 |
| extinction coefficient | 0.016(3) | | 0.0084(10) | 0.0021(3) | 0.0016(3) |

[a] $R_1 = [\sum||F_o| - |F_c||]/\sum|F_o|$; $wR_2 = \{[\sum w[(F_o)^2 - (F_c)^2]^2\}^{1/2}$.

temperature, only a modest of amount of $KNO_3$ oxidant maintained a completely colorless single crystal, eliminating the problem of $V^{5+}$ reduction in both $YVO_4$ and Nd:$YVO_4$ bulk single crystals.[15,18]

In the course of developing a commercially viable growth method, we investigated a number of raw material sources of $YVO_4$ that contained trace amounts of reduced vanadium ions. This was evident in the telltale pale greenish-brown color of the feedstock. Hydrothermal crystal growth using this pale-colored feedstock typically generated colorless, water-clear single crystals of $YVO_4$ along with a trace amount of olive green single crystals of an obviously different morphology mixed in with the target compound. It is clear that the reduced vanadium centers are sequestered to grow in a distinct solid phase, along with the fully oxidized $V^{5+}$ ions in pure $YVO_4$. Tetravalent vanadium $V^{4+}$ adopts the ground state electronic configuration $[Ar]3d^1$ and typically adopts five- or six-coordinate geometries and is characterized by colors in the green/blue range.[19−21]

In this paper, we describe the reaction chemistry and products that result from the sequestration of the reduced vanadium ions into new compounds. In the course of this study, we isolated new interesting minor products and devised new novel synthetic procedures to optimize their yields. Here, we present the synthesis, characterization, and crystal structures of seven new vanadate compounds with their vanadium centers in the $V^{4+}$ oxidation state. These new structures include a hydroxylated metal vanadate with the general formula $A_3VO_5(OH)_3$ (A = Y(**1**), Dy (**2**), or La (**3**)), as well as two phases of nonhydrated $V^{4+}$ vanadates with the general formula $A_2O(VO_4)$ (A = Y (**4**), Dy (**5**; **6**), or Yb (**7**)). The use of hydrazine monohydrate as a reducing agent of $V^{5+}$ to $V^{4+}$ in $YVO_4$ was also examined with the aim of making phase pure hydrated reduced vanadates. Finally, we briefly describe the preparation of several new $V^{5+}$ compounds with the general formula $K_3A(VO_4)_2$ (A = Y, Dy, Ho, Lu, or Yb) that are isolated from related reactions as part of this investigation. These will subsequently be reported in much greater detail.

## EXPERIMENTAL METHODS

**Materials.** All reagents were of analytical grade and used as purchased: $V_2O_5$ (Alfa Aesar, 99.6%), $Y_2O_3$ (Alfa Aesar, 99.9%), $Dy_2O_3$ (Strem, 99.9%), $Yb_2O_3$ (Strem, 99.9%), $La_2O_3$ (Strem, 99.9%), and $N_2H_4{\cdot}H_2O$ (Alfa Aesar). Czochralski grown $YVO_4$ boules were a contribution from Synoptics Crystals in Charlotte, North Carolina.

**2.1. Synthesis.** *Synthesis of $A_3VO_5(OH)_3$ (A = Y (**1**), Dy (**2**), or La (**3**)).* Compounds **1**−**3** were prepared hydrothermally and obtained as side products in the hydrothermal recrystallization of $YVO_4$, $DyVO_4$, or $LaVO_4$ crystals. The vanadate starting materials ($YVO_4$, $LaVO_4$, or $DyVO_4$) were synthesized by stoichiometric solid-state reactions between $V_2O_5$ with $Y_2O_3$, $Dy_2O_3$, or $La_2O_3$ at 900 °C for 9 h or contributed by Synoptics as described above. The $Y_3VO_5(OH)_3$ phase was first observed as a minor product resulting from the hydrothermal recrystallization of light green colored Czochralski grown $YVO_4$ with 2 M NaOH at 560 °C for 4 days. In this reaction, the resulting $YVO_4$ crystals were completely colorless, and the $V^{4+}$ appeared to be completely sequestered in this side product. Alternatively, recrystallization of ∼150 mg of $YVO_4$, $DyVO_4$, or $LaVO_4$ (prepared from the solid-state reactions described above) using 0.4 mL of 1−4 M NaOH at 560 °C for 4 days in weld-sealed silver ampules also resulted in formation of $A(VO_4)$ crystals as the major product and $A_3VO_5(OH)_3$ (A = Y (**2**), Dy


dx.doi.org/10.1021/ic2024132 | Inorg. Chem. 2012, 51, 3588−3596

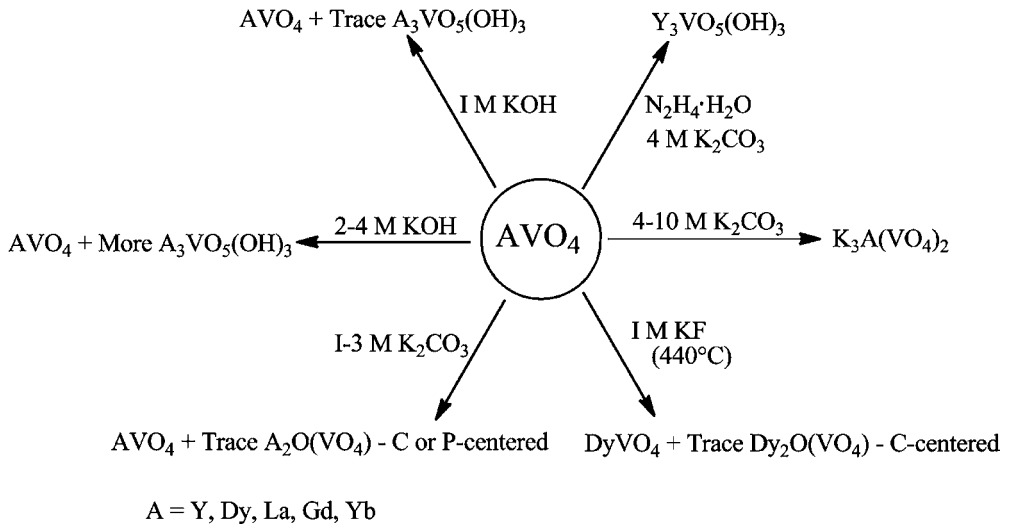


**Figure 1.** Reaction scheme showing the synthesis of hydroxylated and oxy-vanadates at 560 °C and 25 000 psi with exception of C-centered $Dy_2O(VO_4)$ (440 °C). In all cases, the $AVO_4$ starting material contains trace contamination of reduced $V^{4+}$ centers.

(**2**), or La (**3**)) crystals as the minor product. Compounds **1**, **2**, and **3** were subsequently obtained in phase pure yields via a hydrothermal reduction reaction of ~200 mg of $YVO_4$, $DyVO_4$, or $LaVO_4$ using a combination of 0.2 mL of $N_2H_4{\cdot}H_2O$ and 0.3 mL of 4 M $K_2CO_3$ mineralizers at 560 °C for 4 days in weld-sealed silver ampules. After all reactions, the contents of the ampule were filtered and the products washed with deionized water to yield the colorless and/or green hexagonal crystals.

*Synthesis of $A_2O(VO_4)$ (A = Y (**4**), Dy (**5**; **6**), and Yb (**7**)).* Compounds **4**, **5**, and **7** were also obtained as minor products via hydrothermal crystallization of ~150 mg of $YVO_4$, $DyVO_4$, or $YbVO_4$ using 0.4 mL of 4 M $Rb_2CO_3$ or 4 M $K_2CO_3$ at 560 °C for 4 days in weld-sealed silver ampules. After reaction, the reaction products, including the dark blue hexagonal crystals of the title compounds, were manually isolated, washed with deionized water, and air-dried. The predominant product of this reaction was $AVO_4$ (A = Y, Dy, or Yb), but compounds **4**, **5**, and **7** were easily hand-separated by their blue color from the colorless $AVO_4$. The C-centered monoclinic polymorph of compound **6** was also obtained as a fractional product via hydrothermal crystallization of ~150 mg of $DyVO_4$ using 0.4 mL of 2 M KF as a mineralizer at 440 °C for 4 days in weld-sealed silver ampules. The predominant products were again well-formed colorless single crystals of $DyVO_4$.

*Synthesis of $K_3A(VO_4)_2$ (A = Y, Dy, Ho, Lu, or Yb).* As a typical example, the synthesis of $K_3Ho(VO_4)_2$ was accomplished via hydrothermal crystallization of $HoVO_4$ with 4−10 M $K_2CO_3$ at 560 °C in a silver ampule for 6 days. The sealed ampule was loaded into a Tuttle autoclave, which was counter-pressured with additional water. The autoclave was heated at 560 °C for 6 days, typically generating a counter-pressure of 25 200 psi. The contents of the ampule were filtered and the products washed with deionized water to yield phase pure colorless crystals. The other analogs can be prepared in similar fashion.

**X-Ray Diffraction.** Powder X-ray diffraction (PXRD) data were collected using a Rigaku Ultima IV X-ray diffractometer with Cu K$\alpha$ radiation ($\lambda$ = 1.5418 Å). Patterns were collected from 5 to 65° in 2$\Theta$ at a scan speed of 1.0°/min. All single crystal XRD solutions were confirmed using PXRD data and compared to predicted powder patterns simulated from the single crystal data using the Mercury program.[22] Single crystal X-ray intensity data were collected using a Rigaku Mercury CCD detector and an AFC-8S diffractometer equipped with graphite monochromated Mo K$\alpha$ radiation ($\lambda$ = 0.71073 Å). The space groups were determined from the observed systematic absences and confirmed using the MISSYM algorithm within the PLATON program suite.[23] Data reduction, the application of Lorentz and polarization effects, and absorption corrections were performed using the CrystalClear program.[24] The structures were solved by direct methods and refined using subsequent Fourier difference techniques, by full-matrix least-squares, on $F^2$ using SHELXTL 6.10.[25]

All atoms were refined anisotropically with the exception of the hydrogen atoms. In the structures of compounds **1**−**3**, the location of the hydrogen atom was determined by examining both the local geometries of the oxygen environments and the locations of residual electron density. The positions of the hydrogen atoms were restrained to these locations to prevent the O−H bond distance from shortening significantly during subsequent refinements. Data from the single crystal structure refinements of compounds **1**, **4**, **5**, **6**, and **7** are given in Table 1, while those of compounds **2** and **3** can be found in Table S1 in the Supporting Information. All single crystal solutions were confirmed by simulating the powder pattern from the single crystal structure determinations and comparing these to the powder patterns obtained from the bulk reaction products.

**Additional Characterization.** Infrared spectroscopy was performed using the KBr pellet technique under flowing nitrogen with a Nicolet Magna 550 IR spectrometer. Spectra obtained were the average of 16 scans over a 400−4000 $cm^{-1}$ range with a 4 $cm^{-1}$ resolution. Optical spectra of the title compounds were recorded on a PC-controlled SHIMADZU UV-3100/vis/near-IR spectrometer equipped with an integrating sphere. Green crystals of **1** and **2** and blue crystals of **4** were ground and smeared onto $BaSO_4$ plates for data collection. The absorption data were collected in the range of 200−800 nm using a slow scan speed.

## RESULTS AND DISCUSSION

**Synthesis.** This work was initially prompted by our earlier growth studies of $YVO_4$ single crystals. We found that hydrothermal growth leads to high quality, colorless $YVO_4$ single crystals in 1 M $OH^-$ mineralizer. During our earlier detailed crystal growth study, we noticed a small amount of olive green crystals that were often interspersed in the otherwise colorless $YVO_4$ single crystals that formed the bulk of the product. This minor product also formed high quality single crystals and intrigued us because the trace green color in the feedstock had otherwise completely disappeared. Thus, we initially isolated the distinct green side product crystals by hand for preliminary investigations. Single crystal characterization revealed that it is indeed a $V^{4+}$ compound $Y_3VO_5(OH)_3$. Subsequent work demonstrates that this works with a variety of other rare earth elements as well. Materials **1**−**3** crystallized as


dx.doi.org/10.1021/ic2024132 | Inorg. Chem. 2012, 51, 3588−3596

minor products from impure $YVO_4$, $DyVO_4$, and $LaVO_4$, respectively, using 1 M NaOH as the mineralizer, along with high quality single crystals of the majority product $AVO_4$ (A = Y, Dy, or La). Mixtures of $AVO_4$ and relatively increased amounts of $A_3VO_5(OH)_3$ (A = Y (**1**), Dy (**2**), or La (**3**)) were obtained using higher concentrations (2−4 M) of NaOH as the mineralizer (Figure 1). The crystals were easily distinguishable from the main products in their respective reactions based on their morphology and color, olive green for $Y_3VO_5(OH)_3$ (**1**), brown for $A_3VO_5(OH)_3$ (A = Dy (**2**) or La (**3**)), and blue for $A_2O(VO_4)$ (A = Y (**4**), Dy (**5**; **6**), or Yb (**7**)), vida infra.

When carbonates are used as alternative mineralizers, a different $V^{4+}$ species is isolated, namely, $A_2O(VO_4)$. The materials **4**, **5**, and **7** also crystallized as trace products in the presence of high quality crystals of $YVO_4$, $DyVO_4$, and $YbVO_4$, respectively, used when a relatively low concentration of alkali carbonates, 1−3 M $Rb_2CO_3$ or $K_2CO_3$, was used as the mineralizer. A mixture of $AVO_4$ and increased amounts of $A_2O(VO_4)$ (A = Y (**4**), Dy (**5**), or Yb (**7**)) was obtained using 4 M $Rb_2CO_3$ or $K_2CO_3$. When the reactions were extended to use KF as the mineralizer at 440 °C instead of carbonate or hydroxide at 560 °C, trace amounts of yet another material with a $V^{4+}$ ion, C-centered $A_2O(VO_4)$ (**6**), are formed. However, in this case, the alternative polymorph in the $C2/c$ space group is isolated instead of the $P2_1/c$ space group that is obtained using the carbonates (see the Discussion below and Figure 1). These reduced oxyvanadates, **4**−**7**, all have a characteristic blue color. The preferential formation of compounds **1**−**3** from 2 to 4 M hydroxide solutions versus compounds **4**−**7** from 1 to 3 M carbonate solutions or fluoride suggests that this system is particularly sensitive to the nature of the mineralizer ion.

The identification of the trace green product as a $V^{4+}$ compound suggested that the yield of the reduced material could be improved in the presence of a reducing agent.[26] Indeed, this proved to be the case. These compounds, **1**−**3**, were obtained in phase pure yields using a combination of 0.2 mL of $N_2H_4{\cdot}H_2O$ and 0.3 mL of $K_2CO_3$ as the mineralizer. The hydrazine monohydrate in this case was used as a reducing agent in the reduction of $V^{5+}$ to $V^{4+}$, as previously reported.[26]

We find that the $A_2O(VO_4)$ phases (**4**, **5**, **7**) form in trace quantities from impure $YVO_4$ feedstock as the source of the $V^{4+}$ ions when 1−4 M carbonate is employed as the mineralizer. As with KOH mineralizer, the bulk of the reaction product is colorless, high quality $YVO_4$ single crystals, with the $V^{4+}$ species only forming as a minor product. Unlike with the hydroxylated species **1**−**3**, we have thus far been unsuccessful in growing these products in high yield. All attempts to produce pure materials using a reducing agent only lead to the hydroxylated phases **1**−**3**.

Interestingly, when a higher concentration of carbonates is used as the mineralizer (≥4 M $K_2CO_3$), an entirely different material is obtained with the formula $K_3A(VO_4)_2$ (A = Y, Dy, Ho, and Lu). In this case, the compounds contain exclusively $V^{5+}$ vanadate building blocks with no reduced $V^{4+}$ or $V^{3+}$ evident, as demonstrated by the colorless nature of the crystals. These compounds are members of an extensive and fascinating class of structures known as the glaserite phases, with the parent derivative having the formula $K_3Na(SO_4)_2$.[27] Despite the many members of this class of compounds, few exist in the highest symmetry parent form in space group $P\bar{3}m1$.[28,29] The derivatives we isolated here do crystallize in the high symmetry trigonal phase and have considerable potential as new materials. They are the subject of a much more detailed report to be forthcoming.

**Crystal Structures of $A_3VO_5(OH)_3$ (A = Y (1), Dy (2), or La (3)).** Compounds **1**−**3** crystallize in the monoclinic space group $P2_1/m$ (No. 11) and have essentially identical structures despite the choice of rare earth samples with a wide range of ionic radii. Only the yttrium compound (**1**) is discussed in detail as the prototype structure, with the crystal data for the other rare earth analogs available in the Supporting Information Tables S1 and S2. The structures of **1**−**3** resemble those of previously reported hydroxyl and fluoro-germanates such as $Dy_3GeO_5(OH)_3$,[30] $Gd_3GeO_5(OH)_3$,[31] $Sm_3GeO_5(OH)_3$,[32] and $Y_3GeO_5((OH)_{0.5}F_{0.5})_3$.[32] The crystal structures of **1**−**3** have two different coordination sites for their respective $A^{3+}$ (A = Y, La, and Dy) cations, while the vanadium cations are pentacoordinated by five oxygen atoms in a square pyramidal arrangement. The crystal structure of compound **1** contains two crystallographically independent $Y^{3+}$ cations (Figure 2). Y(1) is coordinated by eight oxygen atoms, five of which are also bound to vanadium centers, while the other three are shared only between yttrium atoms. Y(2) is coordinated by seven oxygen atoms, and four of these are vanadium-bonded, while the other three are again only yttrium-bonded. The cations Y(1) and Y(2) have average Y−O bond distances of 2.398 (4) Å and 2.337 (4) Å, respectively, and these average Y−O bond lengths are very similar to those found in $Y_3GeO_5((OH)_{0.5}F_{0.5})_3$ (Y(1) = 2.3944; Y(2) = 2.3297).[32] The atoms Y(1), V(3), O(4), O(5), and H(5) sit on special positions with site symmetry $m$. Coordination about vanadium occurs as square pyramids. Here, the apical V═O bond is much shorter (1.697(5) Å) than the vanadium oxygen distance of the square base (1.926(4) Å; Table 2). The hydrogen atoms in these structures are bound to O(3) and O(5) oxygen atoms, which

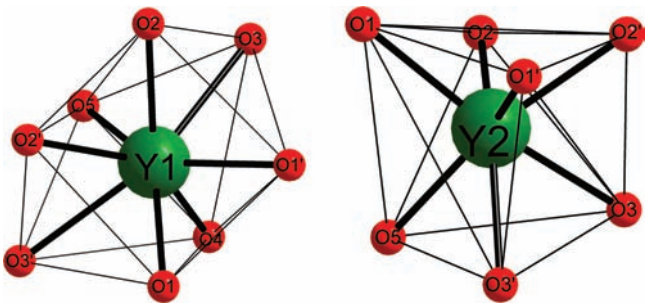


**Figure 2.** Coordination polyhedra of the two crystallographically unique $Y^{3+}$ cations in $Y_3VO_5(OH)_3$ (**1**).

**Table 2. Selected Bond Distances and Angles for Compound 1**

| | | | |
|---|---|---|---|
| Y(1)−O(2) | 2.337(4) | Y(2)−O(5) | 2.472(3) |
| Y(1)−O(1) | 2.344(4) | V(1)−O(4) | 1.697(5) |
| Y(1)−O(4) | 2.369(5) | V(1)−O(2) | 1.907(4) |
| Y(1)−O(5) | 2.378(5) | V(1)−O(2) | 1.907(4) |
| Y(1)−O(3) | 2.539(4) | V(1)−O(1) | 1.946(4) |
| Y(2)−O(2) | 2.222(4) | O(4)−V(1)−O(2) | 108.50(19) |
| Y(2)−O(3) | 2.262(4) | O(2)−V(1)−O(2) | 81.0(2) |
| Y(2)−O(2) | 2.292(3) | O(4)−V(1)−O(1) | 108.02(18) |
| Y(2)−O(1) | 2.293(4) | O(2)−V(1)−O(1) | 86.58(16) |
| Y(2)−O(1) | 2.384(4) | O(2)−V(1)−O(1) | 143.46(15) |
| Y(2)−O(3) | 2.433(4) | O(1)−V(1)−O(1) | 83.2(2) |


dx.doi.org/10.1021/ic2024132 | Inorg. Chem. 2012, 51, 3588−3596

bind to the yttrium or rare earth atoms. The −OH groups are not involved in the reduction of the vanadium site from $V^{5+}$ to $V^{4+}$ but do lead to the overall stabilization of the charge balance of the compound. Hydrogen bonding appears to occur by O5−H5−O4, which adds more stability to the crystal structure and helps satisfy the bond valences of the oxygen atoms.

For the remaining compounds of this structure type, **2** and **3**, A−O bond distances range from 2.329(8) to 2.547(17) Å for A(1) and 2.215(8) to 2.486(11) for A(2), so only a small amount of elongation is observed compared to the Y compound. Likewise, V−O bonds range from 1.915(14) to 1.964(9) Å, and V═O bonds range from 1.670(2) to 1.673(12) Å in these analogs. Thus, a small amount of flexibility in the vanadium oxygen bonds compensates for any differentials in the A−O bonding to account for the highly similar unit cell volumes in compounds **1**−**3**. The selected bond distances and angles for compounds **2** and **3** are presented in Table S3 of the Supporting Information.

The packing diagram of $Y_3VO_5(OH)_3$ (**1**) is shown in Figure 3. Along the *c* axis, the $[YO_7]$ polyhedra are connected by

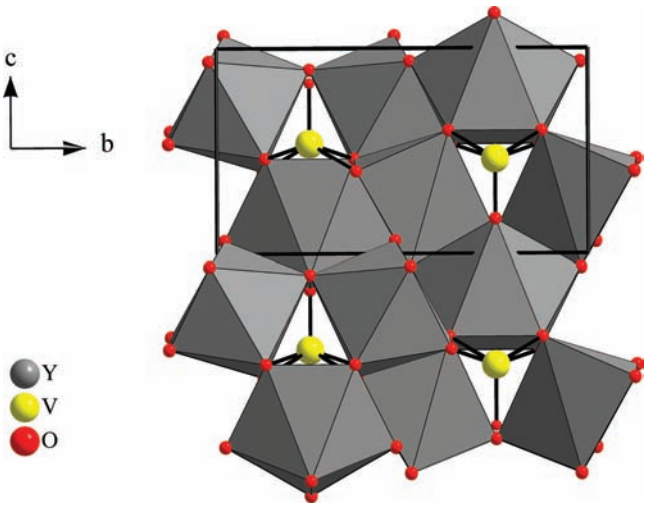


**Figure 3.** Crystal packing diagram of $Y_3VO_5(OH)_3$ (**1**) along the *a* axis.

corner and edge sharing to form a zigzag chain. The $[YO_8]$ polyhedra are edge sharing with the $[YO_7]$ polyhedra and form infinite helical chains along the [010] direction. In combination, these chains form a fairly compact framework structure of Y−O bonding with isolated gaps that are filled by the vanadium polyhedra. The $[VO_5]^{-6}$ square pyramid shares one edge (through a pair of O1 atoms) with a $[YO_8]$ polyhedron and two O2−O2′ edges with $[YO_7]$ polyhedra and is corner sharing with $[YO_7]$ polyhedra through the vanadyl bond approximately along the [001] axis.

**Crystal Structures of Monoclinic $Y_2O(VO_4)$ (4), $Dy_2O(VO_4)$ (6), and $Yb_2O(VO_4)$ (7).** Compounds **4**, **6**, and **7** crystallize in the monoclinic spacegroup *C*2/*c* (No. 15). The crystal structure of these compounds resembles that of high temperature *oxo*-silicates (B-type phase) with the general formula $Ln_2O(SiO_4)$ (Ln = Y and Dy to Lu),[33−36] which themselves crystallize with the $(Mn,Fe)_2[PO_4]F$ structure.[37−39] The $Y^{3+}$ cations in the crystal structures of **4** have crystallographically different coordination numbers of 6 for Y1 and "6 + 1" for Y2. The coordination around Y1 and Y2 in the crystal structure of **4** is shown in Figure 4a, which shows the two

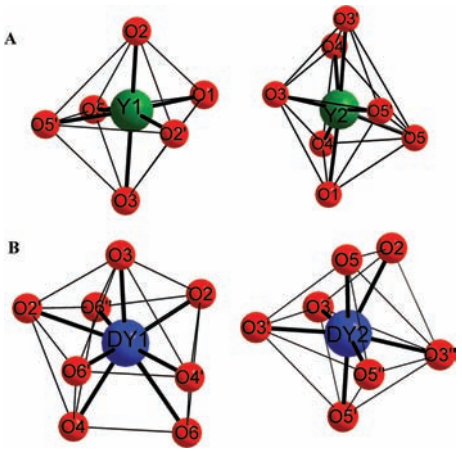


**Figure 4.** Coordination polyhedra of the crystallographically unique $Y^{3+}$ and $Dy^{3+}$ cations in (a) C-centered $Y_2O(VO_4)$ (**4**) and (b) primitive $Dy_2O(VO_4)$ (**5**).

different crystallographic environments for the $Y^{3+}$ cations, while Table 3 gives the selected bond distances for compounds

**Table 3. Selected Bond Distances for Complexes 4, 6, and 7**

| | A = Y | A = Dy | A = Yb |
|---|---|---|---|
| A(1)−O(5) | 2.223(13) | 2.212(14) | 2.168(17) |
| A(1)−O(1) | 2.276(13) | 2.277(13) | 2.255(18) |
| A(1)−O(2) | 2.289(13) | 2.303(13) | 2.228(18) |
| A(1)−O(5) | 2.292(15) | 2.302(14) | 2.288(15) |
| A(1)−O(3) | 2.293(14) | 2.314(14) | 2.257(18) |
| A(1)−O(2) | 2.304(14) | 2.287(13) | 2.261(18) |
| A(2)−O(5) | 2.194(13) | 2.233(14) | 2.150(16) |
| A(2)−O(4) | 2.303(13) | 2.347(13) | 2.297(16) |
| A(2)−O(1) | 2.339(13) | 2.345(15) | 2.283(17) |
| A(2)−O(4) | 2.348(13) | 2.347(13) | 2.276(15) |
| A(2)−O(3) | 2.364(13) | 2.368(13) | 2.333(18) |
| A(2)−O(5) | 2.374(13) | 2.388(13) | 2.367(15) |
| A(2)−O(3) | 2.591(15) | 2.617(13) | 2.597(17) |
| V(1)−O(1) | 1.620(13) | 1.625(15) | 1.60(2) |
| V(1)−O(4) | 1.626(16) | 1.625(14) | 1.609(19) |
| V(1)−O(2) | 1.635(15) | 1.619(13) | 1.649(18) |
| V(1)−O(3) | 1.649(15) | 1.643(15) | 1.650(16) |
| O(1)−V(1)−O(4) | 114.5(7) | 113.3(7) | 115.1(10) |
| O(1)−V(1)−O(2) | 112.0(7) | 111.0(7) | 109.1(10) |
| O(4)−V(1)−O(2) | 107.9(7) | 109.0(7) | 107.0(9) |
| O(1)−V(1)−O(3) | 113.4(8) | 112.4(8) | 113.1(10) |
| O(4)−V(1)−O(3) | 101.1(7) | 102.5(7) | 102.3(9) |
| O(2)−V(1)−O(3) | 107.2(7) | 108.2(7) | 109.9(10) |

**4**, **6**, and **7**. The Y1 cation has Y−O bond distances ranging from 2.2235(13) to 2.3039(15) Å, and its coordination environment can be described as a distorted octahedron comprised of four vanadium bridged oxygen atoms and two yttrium bonded $O^{2-}$ anions. The O−Y1−O angles range from 77.9(5)° to 165.5(5)°, indicating the angular distortion. On the other hand, the coordination polyhedron of the Y2 cation can be described as a capped octahedron with Y−O bond lengths ranging from 2.1944(13) to 2.374(13) Å and a seventh longer bond of 2.5906(15) Å. The O−Y−O bond angles are between 61.9(5)° and 151.6(5)°, and this large angular distortion is due to the long capping oxygen atom. The $[VO_4]^{-4}$ anion adopts a distorted tetrahedral geometry with V−O bond distances and


dx.doi.org/10.1021/ic2024132 | *Inorg. Chem.* 2012, 51, 3588−3596

O−V−O angles ranging from 1.6199(13) to 1.6494(15) Å and 101.1(7) to 114.5(7)°, respectively. The four vanadium bound oxygen atoms coordinate a total of eight yttrium cations: three of the oxygen atoms bridge five $Y^{3+}$ cations, whereas the fourth oxygen atom bridges to three cations. The fifth oxygen atom O5 adopts a distorted tetrahedron $[OY_4]^{+10}$ and is surrounded by four yttrium cations (two Y2 and two Y1). The O5−Y bond distances and Y−O5−Y angles range from 2.194(13) to 2.374(13) Å and 99.0(5)° to 140.9(6)°, respectively.

The crystal structure of **6** is isostructural to that of **4** and contains Dy−O bond distances and O−Dy−O angles in the range of 2.227(11)−2.604(13) Å and 61.5(5)−164.6(4)°, respectively, while the V−O bond lengths and O−V−O bond angles range from 1.615(12) to 1.633(13) Å and 101.9(7) to 114.0(6)°, respectively. The crystal structure of **7** contains Yb−O bond distances and O−Yb−O angles in the range of 2.150(16)−2.596(17) Å and 56.9(5)−167.6(6)°, respectively, while the V−O bond lengths and O−V−O bond angles range from 1.600(2) to 1.651(16) Å and 102.3(9) to 115.0(10)°. In this way, it appears that compound **7**, based on the smallest rare earth cation, exhibits the most structural distortion in terms of variance of bond lengths and angles of these compounds studied. The unit cell parameters in the crystal structures of **4**, **6**, and **7** increase with increased ionic radii, with the *a* and *b* parameters having the most profound changes, whereas the $\beta$ angle stays relatively unchanged at around 122.0°. Similar results, including structural distortions around the silicates, were observed with the B-type ortho-oxosilicates.[34,36]

The packing diagram of $Y_2O(VO_4)$ (Figure 5) shows $[(Y1)O_6]$ and $[(Y2)O_7]$ polyhedra forming infinite helical

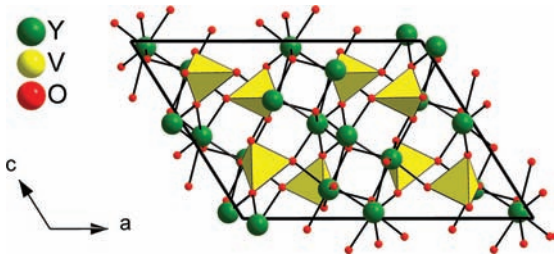


**Figure 5.** Crystal packing diagram of $Y_2O(VO_4)$ (**5**) along the *b* axis.

chains, which propagate by edge sharing. These independent helical chains are connected together by $[VO_4]^{-4}$ tetrahedra. The $[VO_4]^{-4}$ tetrahedra shares corners with three $[(Y2)O_7]$ and four $[(Y1)O_6]$ polyhedra while also edge sharing with the $[(Y2)O_7]$ polyhedron. Tetrahedra of $[OY_4]$ form infinite chains along the *c* axis that are connected along the *b* axis through isolated $[VO_4]^{-4}$ units.

**Crystal Structure of Primitive Monoclinic $Dy_2O(VO_4)$.** Compound **5** crystallizes in the monoclinic spacegroup $P2_1/c$ (No. 14), and its crystal structure resembles that of low temperature *oxo*-silicates (A-type phase) with the general formula $Ln_2O(SiO_4)$ (Ln = Y, La−Gd).[39−43] The crystal structure of compound **5** contains two crystallographically independent $Dy^{3+}$ cations, where Dy(1) is coordinated by eight oxygen atoms: seven of them are vanadium bonded, while one is not (Figure 3b). The Dy1−O bond distances and O−Dy1−O angles range from 2.259(11) to 2.601(12) Å and 58.4(4)° to 159.9(4)°, respectively. The coordination polyhedron around the Dy(2) cation resembles a capped octahedron, where it is coordinated by seven oxygen atoms: four of them are bridged to vanadium, while the other three are bridged to another rare earth. The Dy2−O bond lengths and O−Dy2−O angles range from 2.238(12) to 2.515(14) Å and 63.5(4)° to 170.7(4)°, respectively. The two different crystallographic environments for the $Dy^{3+}$ cations are shown in Figure 4b, while Table 4

**Table 4. Selected Bond Distances for Compound 5**

| | | | |
|---|---|---|---|
| Dy(1)−O(2) | 2.259(11) | Dy(2)−O(3) | 2.477(12) |
| Dy(1)−O(1) | 2.328(12) | Dy(2)−O(3) | 2.514(13) |
| Dy(1)−O(4) | 2.332(13) | V(1)−O(5) | 1.597(14) |
| Dy(1)−O(5) | 2.356(13) | V(1)−O(4) | 1.625(14) |
| Dy(1)−O(4) | 2.435(13) | V(1)−O(3) | 1.640(13) |
| Dy(1)−O(2) | 2.491(13) | V(1)−O(2) | 1.667(13) |
| Dy(1)−O(5) | 2.561(13) | O(5)−V(1)−O(4) | 112.7(7) |
| Dy(1)−O(4) | 2.601(13) | O(5)−V(1)−O(3) | 113.5(7) |
| Dy(2)−O(1) | 2.238(12) | O(4)−V(1)−O(3) | 113.7(7) |
| Dy(2)−O(1) | 2.254(12) | O(5)−V(1)−O(2) | 116.3(7) |
| Dy(2)−O(1) | 2.329(13) | O(4)−V(1)−O(2) | 98.5(7) |
| Dy(2)−O(3) | 2.357(13) | O(3)−V(1)−O(2) | 100.8(6) |
| Dy(2)−O(2) | 2.358(11) | | |

provides selected bond distances. The vanadium atom occupies one crystallographic site with a distorted tetrahedral environment with V−O distances and O−V−O angles ranging from 1.5972 (14) to 1.6664 (13) Å and 98.6(7)° to 113.7(7)°, respectively. We note that this is significantly more distortion than is present in the *C*2/*c* polymorph. The other unique oxygen atom, O3, adopts a distorted tetrahedron $[ODy_4]$ and is surrounded by four dysprosium cations (three Dy2 and one Dy1, also differing from the *C*2/*c* structure type). The O3−Dy bond lengths and Dy−O3−Dy angles range from 2.238(12) to 2.330(14) Å and 100.3(5)° to 127.6(5)°, respectively, which is alternatively a much less distorted environment than is present in the *C*2/*c* polymorph.

The packing diagram of $Dy_2O(VO_4)$ (**5**) results in a three-dimensional framework, as shown in Figure 6. The $[Dy(1)O_8]$

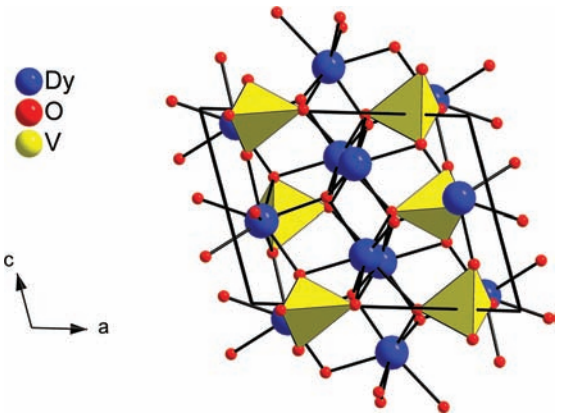


**Figure 6.** Crystal packing diagram of $Dy_2O(VO_4)$ (**5**) along the *b* axis.

polyhedra edge shares to itself, resulting in an infinite helical chain along the *c* axis. These helical $[Dy(1)O_8]$ polyhedral chains are connected together by $[Dy(2)O_7]$ polyhedra that are edge connected and run in a zigzag fashion along the *c* axis. The $[ODy_4]$ tetrahedron shares a common edge with another $[ODy_4]$ tetrahedron and corners with four other $[ODy_4]$ tetrahedra. Along the *a* axis, these $[ODy_4]$ tetrahedra are connected together via isolated $[VO_4]^{-4}$ units. It is interesting that this structure type was only obtained for the Dy compound


dx.doi.org/10.1021/ic2024132 | Inorg. Chem. 2012, 51, 3588−3596

Table 5. Different $V^{4+}$ Coordination Geometries and Varied V−O Bond Distances and O−V−O Bond Angles in Compounds 1, 4, and 5

| compound | S.G. | $V^{4+/5+}$ geometry | V−O bond lengths (Å) | O−V−O bond angles |
|---|---|---|---|---|
| $Y_3VO_5(OH)_3$ (**1**) | $P2_1/m$ | distorted square pyramidal | 1.697(5)−1.946(4) Å V=O 1.697(5) | 81.0(2)−143.46(15)° |
| $Y_2O(VO_4)$ (**5**) | $C2/c$ | distorted tetrahedral | 1.6199 (13)−1.6494 (15) Å | 101.1(7)−114.5(7)° |
| $Dy_2O(VO_4)$ (**6**) | $P2_1/c$ | distorted tetrahedral | 1.5972(14)−1.6664(13) Å | 98.6(7)−113.7(7)° |

in this study and not for the smaller rare earth cations. As with the *oxo*-silicates, it appears that Dy is near the boundary of where the A- and B-type crystal structures are stable.

**Comparative $V^{4+}$ Coordination Geometry.** The coordination geometries of the vanadium atoms in all of these species deserve comment, as they differ greatly in the three structure types, as shown in Table 5. Coordination about vanadium in **1**−**3** occurs in a vanadyl [1 + 4]-coordination as distorted $[VO_5]^{-6}$ square pyramids. Here, the apical V=O bond is much shorter than the four equatorial vanadium−oxygen bond distances on the square base. The vanadyl ion in **1** has a bond length of 1.697(6) Å, while the average V−O bond distance within the square base is 1.926(4) Å. It is worth noting that such a vanadyl bond distance of 1.697(6) Å in **1** is rare and noticeably longer compared to typically observed vanadyl bonds in the range of 1.56−1.62 Å.[20] The equatorial V−O bonds of **1** in the range of 1.907(4)−1.946(4) Å are in fact marginally shorter than what is most commonly observed (1.94−2.02 Å) in a square pyramidal geometry but are not nearly as uncommon in this respect as the observed vanadyl distance.[20] Despite these extremes, the O=V−O angles fall right within the target range for this geometry (100−110°). Average O=V−O bond angles are 108.26°, and O−V−O bond angles of the distorted base range from 81.04 to 86.58° with O−V−O angles of 143.46° spanning the base. Interestingly, in compounds **4** (space group $C2/c$) and **5** (space group $P2_1/c$), the $V^{4+}$ cation adopts a distorted tetrahedral geometry with one V−O bond longer than the other three in the $VO_4$ polyhedra. Tetrahedral coordination is quite rare for $V^{4+}$ ions, and only two examples of tetrahedrally coordinated tetravalent vanadium have been reported, namely, $Ba_2VO_4$ and $\beta$-$Sr_2VO_4$.[44,45] Like compounds **4**−**7** and their corresponding oxo-silicates, these tetrahedral alkaline earth vanadates ($Ba_2VO_4$ and $\beta$-$Sr_2VO_4$) also have direct silicate analogs with the general formula $M_2SiO_4$ (M = Ca, Sr, Ba).[46−48] This suggests that perhaps the tetrahedral $V^{+4}$ coordination is only stabilized by the lattice environment. The V−O bond distances in **4** (1.6199(13)−1.6494 (15) Å) and **5** (1.5972(14)−1.6664(13) Å) are shorter compared to those found in $Ba_2VO_4$ (1.73(3)−1.83(3) Å) and $\beta$-$Sr_2VO_4$ (1.65(3)−1.88(3)).[44] It is also worthwhile noting that the O−V−O angles in **4** and **5** are very similar to those found in $Ba_2VO_4$ (98.6(3)−114.4(15)°) but are less distorted than those observed in $\beta$-$Sr_2VO_4$ (100(1)−126(1)°).[44]

**Infrared Spectroscopy.** Infrared spectroscopy was used to probe the coordination geometry of the vanadium cation in the reported compounds. Figure 7 shows the infrared spectra of $Y_3VO_5(OH)_3$ (**1**) and $Y_2O(VO_4)$ (**4**). The IR spectrum of **1** has seven different absorptions ranging from 422 to 3580 $cm^{-1}$. The absorption peaks between 422 and 580 $cm^{-1}$ correspond to the stretching vibrations of $\nu$(V−O−V).[49] The peak at 751 $cm^{-1}$ can be attributed to $\nu$(V−O),[50] of four V−O single bonds with bond lengths of 1.904(11) × 2 and 1.930(11) × 2 Å, whereas the absorption peak at 868 $cm^{-1}$ is probably due to $\nu$(V=O). Typically, vanadyl vibrational stretches are found in the range of 950−1050 $cm^{-1}$, but the location of $\nu$(V=O) in **1** is consistent with a weaker (longer) vanadyl bond of 1.690(17) Å compared to that of a more typical distance of 1.58 Å in $V_2O_5$.[19,20,51] The remaining two absorption peaks at 3474 and 3580 $cm^{-1}$ most likely belong to the two crystallographically different O−H bonds found in the unit cell of $Y_3VO_5(OH)_3$. The IR spectrum of $Y_2O(VO_4)$ (**4**) contains three distinct peaks at 451, 596, and 823 $cm^{-1}$. The peaks at 451 and 596 $cm^{-1}$ most likely correspond to stretching vibrations of $\nu$(V−O−V), while those of $\nu$(V−O) are found at 823 $cm^{-1}$.[52]

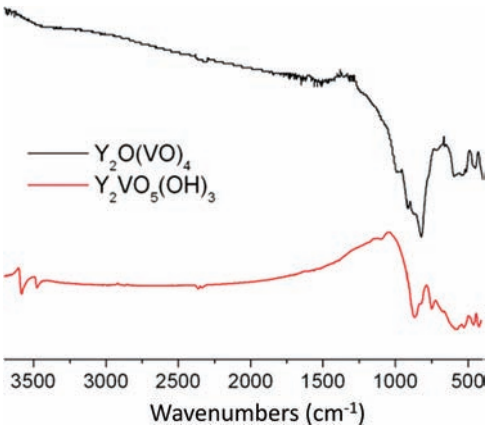


Figure 7. IR spectra of $Y_2O(VO_4)$ (**4**; top) and $Y_2VO_5(OH)_3$ (**1**; bottom).

**Optical Properties of the New Vanadate Compounds 1 and 4.** The absorption spectra of compounds **1** and **4** are shown in Figure 8, while that of **2** can be found in Supporting Information Figure S1. The absorption peaks in $Y_3VO_5(OH)_3$ (**1**) are centered at 682, 497, 349, and 222 nm, while those in $Y_2O(VO_4)$ (**4**) are found at 641, 353, and 250 nm. The dysprosium compound $Dy_3VO_5(OH)_3$ (**2**) has corresponding peak maxima at 642, 449, and 273 nm. For all of the compounds above the absorption peaks below 500 nm are attributed to excitation between $V_{3d}$ and $O_{2p}$ electronic states,[53,54] while those in the range of 641−682 nm may be due to $V^{4+}$ d−d transition or a charge transfer band.[55] The broad absorption peak (Figure 7 right) at 682 nm provides the olive green color in compound **1**, whereas the blue color of **4** results from the broad peak at 641 nm.

## CONCLUSIONS

We report here a series of chemical reactions that began as an attempt to characterize the proposed $V^{4+}$ impurities in $YVO_4$ single crystals and related analogs. The chemistry proved much richer than we anticipated, and we currently have seven new $V^{4+}$-containing compounds that have been synthesized hydrothermally and characterized using single crystal X-ray diffraction, powder diffraction, and infrared and absorption spectroscopy. All of the compounds result from the reactions of various mineralizers reacting with the well-known $AVO_4$ phase that invariably contains a trace amount of $V^{4+}$ impurity in the crystal lattice. The $V^{4+}$ ions can be sequestered and isolated as a


dx.doi.org/10.1021/ic2024132 | Inorg. Chem. 2012, 51, 3588−3596

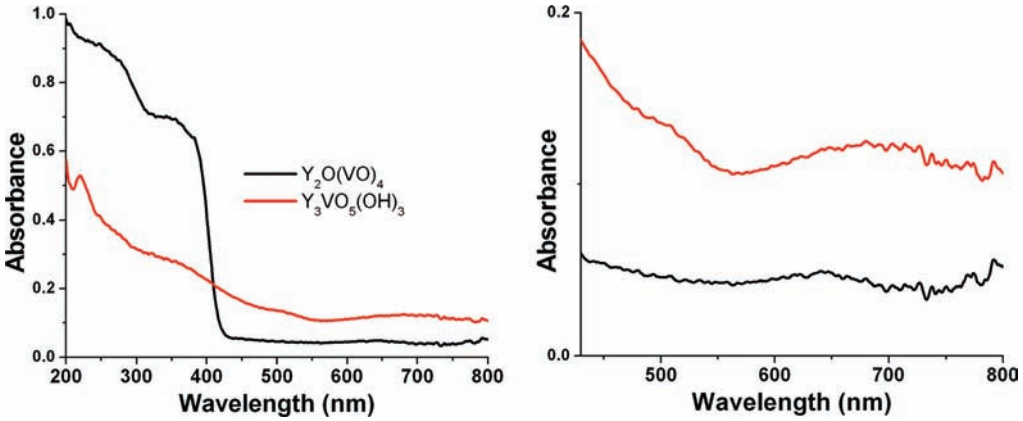


**Figure 8.** Absorption spectra of compounds **1** and **4** (left) and zoomed-in broad absorption peaks of the same compounds in the range of 435−800 nm (right).

trace amount of well-formed single crystals in all cases. Thus, use of $OH^-$ as mineralizer with pale green $AVO_4$, contaminated with trace amounts of $V^{4+}$, leads to the formation of $A_3VO_5(OH)_3$ (A = Y, Dy, and La), compounds **1**−**3**, respectively. The amounts of **1**−**3** increase relative to the parent $AVO_4$ as the concentration of $OH^-$ mineralizer increases but still remains as a minor product relative to the $AVO_4$ main product. These compounds can be grown phase pure by use of the reducing agent hydrazine monohydrate and 4 M $K_2CO_3$ mineralizer as well formed single crystals in hydrothermal solutions. In all of the hydroxylated rare earth $V^{4+}$ vanadate compounds, the vanadyl state is clearly observed both crystallographically and through electronic and vibrational spectroscopy. Compounds **1**−**3** represent the first reported single crystal structures of hydroxylated rare earth vanadates with the general formula $A_3VO_5(OH)_3$ (A = Y, Dy, and La), so this constitutes a significant new addition to the descriptive chemistry of rare earth vanadates.

When the mineralizer is changed to modest concentrations of carbonate, such as 1−2 M $K_2CO_3$ under similar conditions, the primary product is still $AVO_4$ but the $V^{4+}$ impurity is now sequestered as a new rare earth C-centered monoclinic oxovanadate $A_2O(VO_4)$. These are structurally similar to a well-known series of orthosilicates $A_2O(SiO_4)$ that are used as hosts for scintillators in medical imaging and nuclear physics. Interestingly, in the particular case of Dy, when the mineralizer is changed to fluoride KF, a different polymorph in C-centered monoclinic phase of $Dy_2O(VO_4)$ (**6**) can be isolated. This also has a silicate analog as well. Both of these compounds also contain the rare $[VO_4]^{4-}$ tetrahedral geometry for $V^{4+}$. Finally, when increased amounts of carbonate are used as the mineralizer (≥4 M $K_2CO_3$), the $YVO_4$ feedstock begins to get attacked and no longer recrystallizes as the parent compound. Instead, a new $V^{5+}$-containing phase is isolated with the formula $K_3Y(VO_4)_2$. This compound assumes the high symmetry glaserite structure with $Y^{3+}$ in a crystallographic octahedral site with tetrahedral $VO_4^{3-}$ building blocks. This intriguing new material has considerable potential as a new laser host and will be the subject of an upcoming report.

## ■ ASSOCIATED CONTENT

### Supporting Information

An absorption spectrum, a packing diagram, tables of crystallographic information and bond distances, and crystallographic information in .txt format. This material is available free of charge via the Internet at http://pubs.acs.org.

## ■ AUTHOR INFORMATION

### Corresponding Author

*E-mail: kjoseph@clemson.edu.

## ■ ACKNOWLEDGMENTS

We are indebted to the National Science Foundation (DMR-0907395) for funding and support.

## ■ REFERENCES

(1) Li, G.; Yao, B. Q.; Meng, P. B.; Duan, X. M.; Ju, Y. L.; Wang, Y. Z. *Opt. Mat.* **2011**, *33*, 937−941.
(2) Meng, X.; Zhu, L.; Zhang, H.; Wang, C.; Chow, Y. T.; Lu, M. *J. Cryst. Growth* **1999**, *200*, 199−203.
(3) Fields, R. A.; Birnbaum, M.; Fincher, C. L. *Appl. Phys. Lett.* **1987**, *51*, 1885−1886.
(4) Zayhowski, J. J.; Dill, C. *Opt. Lett.* **1995**, *20*, 716−718.
(5) Bass, M. *IEEE J. Quantum Electron.* **1975**, *11*, 938−939.
(6) *The Physics and Engineering of Solid State Lasers*; Kalisky, Y., Ed.; SPIE Press: Bellingham, WA, 2006.
(7) Lupei, V.; Pavel, N.; Sato, Y.; Taira, T. *Opt. Lett.* **2003**, *28*, 2366−2368.
(8) Higuchi, M.; Shimizu, T.; Takahashi, J.; Ogawa, T.; Urata, Y.; Miura, T.; Wada, S.; Machida, H. *J. Cryst. Growth* **2005**, *283*, 100−107.
(9) Sohn, K.-S.; Zeon, I. W.; Chang, H.; Lee, S. K.; Park, H. D. *Chem. Mater.* **2002**, *14*, 2140−2148.
(10) Xu, Z.; Kang, X.; Li, C.; Hou, Z.; Zhang, C.; Yang, D.; Li, G.; Lin, J. *Inorg. Chem.* **2010**, *49*, 6706−6715.
(11) Katsumata, T.; Takashima, H.; Ozawa, H.; Matsuura, K.; Nobe, Y. *J. Cryst. Growth* **1995**, *148*, 193−196.
(12) Erdei, S. *J. Cryst. Growth* **1993**, *134*, 1−13.
(13) Oka, K.; Unoki, H.; Shibata, H.; Eisaki, H. *J. Cryst. Growth* **2006**, *286*, 288−293.
(14) Erdei, S.; Klimkiewicz, M.; Ainger, F. W.; Keszei, B.; Vandlik, J.; Suveges, A. *Mater. Lett.* **1995**, *24*, 301−306.
(15) Forbes, A. R.; McMillen, C. D.; Giesber, H. G.; Kolis, J. W. *J. Cryst. Growth* **2008**, *310*, 4472−4476.
(16) Chirayil, T.; Zavalij, P. Y.; Whittingham, M. S. *Chem. Mater.* **1998**, *10*, 2629−2640.
(17) Byrappa, K.; Yoshimura, M. In *Handbook of Hydrothermal Technology*; Noyes Publishers: Park Ridge, NJ, 2001; pp 562−572.
(18) Kolis, J. W. U.S. 7211234, May 1, 2007.
(19) Selbin, J. *Chem. Rev.* **1965**, *65*, 153−175.
(20) Schindler, M.; Hawthorne, F. C.; Baur, W. H. *Chem. Mater.* **2000**, *12*, 1248−1259.

(21) Debbie, C. C.; Alan, S. T. *The Chemistry of Vanadium in Aqueous and Nonaqueous Solution*; American Chemical Society: Washington, DC, 1998; pp 2−29.
(22) Macrae, C. F.; Bruno, I. J.; Chisholm, J. A.; Edgington, P. R.; McCabe, P.; Pidcock, E.; Rodriguez-Monge, L.; Taylor, R.; van de Streek, J.; Wood, P. A. *J. Appl. Crystallogr.* **2008**, *41*, 466−470.
(23) Spek, A. L. *J. Appl. Crystallogr.* **2003**, *36*, 7−13.
(24) *CrystalClear*; Rigaku/MSC: The Woodlands, TX; Rigaku Corporation: Tokyo, Japan, 2006.
(25) Sheldrick, G. M. *Acta Crystallogr.* **2008**, *A64*, 112−122.
(26) Son, J.-H.; Wei, J.; Cobden, D.; Cao, G.; Xia, Y. *Chem. Mater.* **2010**, *22*, 3043−3050.
(27) Okada, K.; Ossaka, J. *Acta Crystallogr., Sect. B* **1980**, *36*, 919−921.
(28) Moore, P. B. *Am. Mineral.* **1973**, *58*, 32−42.
(29) Moore, P. B.; Araki, T. *Am. Mineral.* **1972**, *57*, 1355−1374.
(30) Mamin, V. F.; Halikov, R. A.; Demjanets, L. N.; Golyshev, V. M.; Shibanova, T. A. *Kristallografiya* **1987**, *32*, 878−881.
(31) Genkina, E. A.; Demyanets, L. N.; Mamin, B. F.; Maximov, B. A. *Kristallografiya* **1989**, *34*, 1002−1005.
(32) Golovastikov, N. I.; Belov, N. V. *Kristallografiya* **1982**, *27*, 1087−1089.
(33) Smolin, Y. I.; Tkachev, S. P. *Sov. Phys. Crystallogr.* **1969**, *14*, 14.
(34) Smolin, Y. I. *Kristallografiya* **1969**, *14*, 985−989989.
(35) Vanhal, H. A. M.; Hintzen, H. T. *J. Alloy. Compd.* **1992**, *179*, 77−85.
(36) Phanon, D.; Cerny, R. *Z. Anorg. Allg. Chem.* **2008**, *634*, 1833−1835.
(37) Rea, J. R.; Kostiner, E. *Acta Crystallogr.* **1972**, *B 28*, 2525−2529.
(38) Waldrop, L. *Z. Kristallogr.* **1969**, *130*, 1.
(39) Wang, J.; Tian, S.; Li, G.; Liao, F.; Jing, X. *Mater. Res. Bull.* **2001**, *36*, 1855−1861.
(40) Fukuda, K.; Iwata, T.; Champion, E. *Powder Diffr.* **2006**, *21*, 300−303.
(41) Gustafsson, T.; Klintenberg, M.; Derenzo, S. E.; Weber, M. J.; Thomas, J. O. *Acta Crystallogr., Sect. C* **2001**, *57*, 668−669.
(42) Maksimov, B. A.; Ilyukhin, V. V.; Kharitonov, Y. A.; Belov, N. V. *Kristallografiya* **1970**, *15*, 926−933933.
(43) Muller-Bunz, H.; Schleid, T. *Z. Anorg. Allg. Chem.* **1999**, *625*, 613−618.
(44) Liu, G.; Greedan, J. E. *J. Solid State Chem.* **1993**, *103*, 228−239.
(45) Gong, W.; Greedan, J. E.; Liu, G.; Bjorgvinsson, M. *J. Solid State Chem.* **1991**, *95*, 213−219.
(46) Catti, M.; Gazzoni, G.; Ivaldi, G. *Acta Cryst. C* **1983**, *39*, 29−34.
(47) Jost, K. H.; Ziener, B.; Seydel, R. *Acta Cryst. B* **1977**, *33*, 1696−1700.
(48) Pieper, G.; Eysel, W.; Hahn, T. *J. Am. Ceram. Soc.* **1972**, *55*, 619−622.
(49) de Waal, D.; Heyns, A. M. *Mater. Res. Bull.* **1992**, *27*, 129−136.
(50) Bi, C. Z.; Ma, J. Y.; Yan, J.; Fang, X.; Yao, D. Z.; Zhao, B. R.; Qiu, X. G. *Eur. Phys. J. B* **2006**, *51*, 167−171.
(51) Botto, I. L.; Vassallo, M. B.; Baran, E. J.; Minelli, G. *Mater. Chem. Phys.* **1997**, *50*, 267−270.
(52) Liming, S.; Xian, Z.; Yanlu, L.; Pan, L.; Honggang, S.; Xiufeng, C.; Weiliu, F. *J. Appl. Phys.* **2010**, *108*, 093519−093528.
(53) Cao, J.; Choi, J.; Musfeldt, J. L.; Lutta, S.; Whittingham, M. S. *Chem. Mater.* **2004**, *16*, 731−736.
(54) Liu, X.; TÃschner, C.; Leonhardt, A.; RÃmmeli, M. H.; Pichler, T.; Gemming, T.; BÃchner, B.; Knupfer, M. *Phy. Rev. B.* **2005**, *72*, 115407.
(55) Taran, M. N.; Langer, K.; Geiger, C. A. *Phys. Chem. Miner.* **2002**, *29*, 362−368.